Direct model predictive speed control strategy for a PMSM fed by a three-level NPC converter

SAJAD SABERI[1] **AND BEHROOZ REZAIE**[1,*]

[1] *Faculty of Electrical Engineering, Babol Noshirvani University of Technology, Mazandaran, Babol, Iran*
[*] *Corresponding author: brezaie@nit.ac.ir*

Manuscript received 26 June, 2020; revised 02 October, 2020; accepted 23 October, 2020. Paper no. JEMT-2006-1246.

This paper presents a direct predictive speed control strategy to control a permanent magnet synchronous motor (PMSM) fed by a three-level neutral-point clamped converter (NPC). A new cost function is proposed by incorporating the speed dynamic, the current dynamic and the system constraints to have a good performance without additional outer-loop PI speed controller. The current dynamic added to cost function is based on the concept of the sliding mode control (SMC). Moreover, a load torque observer is used for better performance of the proposed method and the stability of the observer is presented. By combining new reference value of the current into the cost function, the necessity to multiple horizon in the predictive speed control (PSC) is obviated, the effects of the current dynamic on the transient conditions is considered so current distortion and torque fluctuation is reduced considerably and the controller acts as fast as an original direct speed control without cascade structure. Simulation results using MATLAB/SIMULINK demonstrate the performance of the proposed scheme.

keywords: *Model Predictive Control, Sliding Mode Control, Three-Level NPC, Permanent Magnet Synchronous Motor.*

http://dx.doi.org/10.22109/jemt.2020.236813.1246

NOMENCLATURE

$i_a\ i_b\ i_c$ PMSM 3 phase stator current
V_{DC} DC Link voltage
C DC Link capacitor (F)
V_O Neutral point voltage
R_S PMSM Stator
L_S PMSM stator inductance
$L_d\ L_q$ PMSM inductances of d and q axis
Z_p Number of pole pairs
J_m Motor inertia
B_v Friction coefficient
Ψ_{mg} PMSM flux linkage
T_L Load torque
P_i Probability of the occurrence of the cluster i
S_a, S_b, S_c Switching state of three phases
T_s Sampling time
V_d, V_q PMSM voltages in d and q axis

1. INTRODUCTION

PMSMs have been widely applied in many applications such as electric vehicles, wind turbine, robot manipulators and industrial equipment. This wide variety of usage is because of the advantages of the PMSM such as fast dynamic response due to its low inertia, high power density, high efficiency and accurate speed/position tracking compared with the induction motors [1, 2].

There are many control methods for PMSMs. Among them, the field oriented control (FOC) and direct torque control (DTC) are the most common strategies [3, 4]. Windup problem, mutual impact of controlled variables and bandwidth limitation lead to some difficulties in the FOC schemes [5]. The DTC utilizes switching-table to directly control the motor torque. Since the output voltage vectors are not always optimal, this method suffers from high torque and stator flux ripples [6, 7].

One of the effective methods for controlling PMSMs, is model predictive control (MPC) which is of great interest in recent years for many industrial applications [8–11]. Simple treatment of constraints, multivariable structure, and ability of dead time compensation makes MPC one of the best choices for drive systems [12–15]. There are two main categories for the MPC, i.e., continuous control set MPC (CCS-MPC) and finite control set MPC (FCS-MPC) [5, 16]. The former one needs a modulator to

generate gate signals, while the latter one takes advantage of the fact that the number of possible switching states are limited, and thereby it is possible to predict the effects of each voltage space vector (VSV) to determine the best VSV for the next sampling time [17].

FCS-MPC has been used to control the current [16–18] and torque of AC machines as predictive torque control (PTC) in several converter topologies [19, 20]. In most topologies, there is a cascade structure for the speed control. In [21], a predictive speed controller along with a proportional-integral (PI) controller have been analyzed, in which the cascade PI controller delivers the current/torque reference to an inner current control loop.

Direct predictive speed control (DPSC) without the cascade structure is also possible as explained in [22, 23]. In [23], a DPSC strategy for the two-mass system is discussed in which a higher bandwidth speed control than the classical strategies has been provided. In [24], a single optimization algorithm without the cascade structure has been employed to generate the control action for the direct speed control purpose.

Comparing to the current dynamic, the mechanical dynamic is sluggish and this difference between the time constants enforce the designer to consider a longer prediction horizon for DPSC [25]. Moreover, elimination of the outer PI controller not only brings the stability issues, but also decreases the system performance and causes the steady state error [26]. In [27], the authors proposed a new DPSC method by introducing a cost function related to the speed and current dynamics. To achieve better performance, the current reference is constructed based on the speed tracking error and its integral in discrete manner.

In this paper, we propose a DPSC structure to tackle the aforementioned problems. A new cost function is introduced, by incorporating the speed and current dynamics and the system constraints, to have a superior response without additional PI speed controller. To have both benefits of the direct and indirect speed control schemes, we construct the current reference value based on the concept of the sliding mode control (SMC) and apply it to the MPC controller. Therefore, not only stability is considered in the presence of the mechanical model uncertainties, but also the advantages of the MPC is fulfilled.

By considering new reference value of the current in the cost function, necessity to multiple horizon in the PSC is obviated, effects of the current dynamic under the transient conditions is considered and the controller acts as fast as an original direct speed control without the cascade PI controller. Moreover, because of the inherent robust capability of the SMC, the controller has better performance in the presence of the mechanical uncertainties.

This paper proceeds as follows. The models of the motor and convertor are discussed in Section 2. Section 3 presents the procedure of cost function formation and current reference. In Section 4, the load torque and speed observation and their effects on speed prediction are discussed. Finally, the effectiveness of the method is verified by comparing the simulation results with a newly developed PSC method, in Section 5.

2. MOTOR AND INVERTER MODEL DESCRIPTION

Fig.1 shows the PMSM and three-level NPC inverter. Continuous model of a surface-mounted PMSM in rotor flux orientation is as Eq. (1) [26] and parameters are described in nomenclature section.

Table 1. The switching states of one phase of three-level NPC inverter

S_x	S_{x1}	S_{x2}	S_{x3}	S_{x4}	U_x
$P \approx 1$	1	1	0	0	$V_{DC}/2$
0	0	1	1	0	0
$N \approx -1$	0	0	1	1	$V_{DC}/2$

$$\begin{aligned}
\frac{di_d}{dt} &= \frac{1}{L_d}\left(v_d - R_s i_d + \omega_e L_q i_q\right) \\
\frac{di_q}{dt} &= \frac{1}{L_q}\left(v_q - R_s i_q - \omega_e L_d i_d - \omega_e \psi_{mg}\right) \\
\frac{d\omega_e}{dt} &= \frac{Z_p}{J_m}\left(\frac{3}{2} Z_p \psi_{mg} - \frac{B_v}{Z_p}\omega_e - T_L\right)
\end{aligned} \tag{1}$$

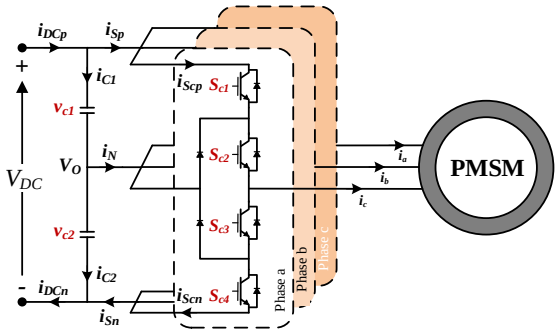

Fig. 1. The PMSM and NPC inverter topology.

Furthermore, v_d and v_q are the voltage vectors in d-q reference frame that are associated with switching states, $U = \begin{bmatrix} U_a & U_b & U_c \end{bmatrix}^T$

$$\begin{aligned}
v_{dq} &= \begin{bmatrix} v_d & v_q \end{bmatrix}^T = MDU \\
M &= \begin{bmatrix} \cos\theta & -\sin\theta \\ \sin\theta & \cos\theta \end{bmatrix} \\
D &= \frac{2}{3}\begin{bmatrix} 1 & -1/2 & -1/2 \\ 0 & \sqrt{3}/2 & -\sqrt{3}/2 \end{bmatrix}
\end{aligned} \tag{2}$$

where D is Clarke transformation matrix, M is Park transformation matrix and θ is the electrical angle of the rotor [27]. Moreover, U is the output voltage of the inverter and can be expressed as function of the capacitor voltage,V_{dc} and switching state, S, i.e. :

$$U_x = \frac{S_x\left(S_x+1\right)}{2} v_{C1} + \frac{S_x\left(S_x-1\right)}{2} v_{C2} \tag{3}$$

where S_x is switching the state variable for phase x with x=a,b,c, and it has three possible values, i.e., $S_x = \{N, 0, P\}$ or $S_x = \{-1, 0, +1\}$ that represents $\{-\frac{V_{DC}}{2}, 0, +\frac{V_{DC}}{2}\}$ voltages.

Table 1 shows all possible switching states. To prevent DC link capacitor short circuit, $S_{x3} = 1 - S_{x1}$ and $S_{x4} = 1 - S_{x2}$.

A discrete model of PMSM is needed for FCS-MPC. When we have high calculation burden, a simple discretizing method with good performance should be selected. Here, the model discretized using Euler method [28] as Eq. (4) and (5).

$$\frac{dx(t)}{dt} = \frac{x(t) - x(t-1)}{T_s} \tag{4}$$

where T_s is sampling time.

$$\begin{aligned} i_d[k+1] &= \left(1 - \tfrac{T_s R_s}{L_s}\right) i_d[k] + \tfrac{T_s}{L_s} v_d[k] \\ &\quad + T_s \omega_e[k]\, i_q[k] \\ i_q[k+1] &= \left(1 - \tfrac{T_s R_s}{L_s}\right) i_q[k] + \tfrac{T_s}{L_s} v_q[k] \\ &\quad - T_s \omega_e[k]\, i_q[k] - \tfrac{T_s \psi_{mg}}{L_s} \omega_e[k] \\ \omega_e[k+1] &= \left(1 - \tfrac{T_s B_v}{Z_p}\right) \omega_e[k] \\ &\quad + T_s \left(\tfrac{3}{2} Z_p \psi_{mg} i_q[k] - T_L\right) \end{aligned} \tag{5}$$

Keeping the neutral point voltage V_o at zero is very important, because the voltage unbalance has negative impact on the output voltage and the semiconductor switch stress [27]. FCS-MPC has the ability to control V_o by designing a factor of this item in cost function. We can predict the voltage of the neutral point by measuring three-phase currents and switching states as follows [29]:

$$\begin{aligned} \tfrac{dV_O}{dt} &= \tfrac{dV_{c1}}{dt} - \tfrac{dV_{c2}}{dt} = \tfrac{1}{C}\left\{\left(I_{Sp} - I_{Sn}\right)\right\} \\ V_O[k+1] &= V_O[k] + \tfrac{T_s}{C}\left(I_{Sp}[k] - I_{Sn}[k]\right) \end{aligned} \tag{6}$$

3. COST FUNCTION AND CURRENT REFERENCE FORMATION

In the conventional DPSC, the reference speed ω_e^* is compared with the predicted speed ω_e^p and the optimal voltage vector will be selected when the error is minimum. As the dynamic of speed is very slow compared to current dynamic, for better performance, the MPC needs a longer prediction horizon [25]. Regardless of the horizon, outer controller is needed to provide the current reference so that increase the robustness of the system against the model inaccuracy.

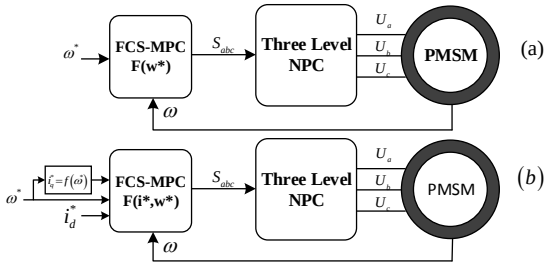

Fig. 2. (a) The conventional speed control system, (b) The direct speed control system.

By incorporating the current and speed dynamic in the single cost function, the controller has the advantages of both direct and indirect speed control schemes and performs good transient response while the robustness against the model uncertainty is achievable.

To choose the combination of switches which is optimal to exert to inverter, the MPC needs a cost function. Our cost function has three parts. C_Z is the part that should drive to zero, C_T describes tracking variables and C_C is constraint part. The zero part includes the neutral point voltage and an equation for maximum torque per ampere (MTPA) criteria [30, 31], and the tracking part includes the speed and q-axis current errors:

$$\begin{aligned} C_Z &= \lambda_{np}(v_{C1} - v_{C2})^2 + \lambda_{id}\left(i_d + \tfrac{L_d - L_q}{\lambda}\left(i_d^2 - i_q^2\right)\right)^2 \\ C_T &= \lambda_\omega(\omega^* - \omega)^2 - \lambda_{iq}\left(i_q^* - i_q\right)^2 \end{aligned} \tag{7}$$

It is worth mentioning that in case of surface-mounted PMSM with $L_d = L_q$, the MTPA parts changes to $\lambda_m(i_d)^2$.

Constraint part can have multiple variables such as the current and switching frequency limitations. Here, we just consider the current limitation I_m. In case of the cascade scheme, the current limitation should be considered in outer loop with PI controller and saturate the control signal. However, in the direct speed control, constraints are considered in the cost function [27].

$$C_R = \begin{cases} \lambda_{\mathrm{I}_m}\left(\sqrt{i_d^2 + i_q^2} - I_m\right) & if\ \sqrt{i_d^2 + i_q^2} > I_m \\ 0 & o.w \end{cases} \tag{8}$$

In the ordinary PSC, only the speed dynamic takes place in the tracking part and because of the difference between the speed and current dynamics, when the speed reaches at its reference, CT will be significantly low. If the prediction horizon is not long enough to consider fast dynamics, high frequency components are generated in the motor currents [23].

In order to alleviate this high frequency component, a combination of SMC with MPC is considered in which the SMC generates a reference value of q-axis current for the cost function of the MPC. Thus, we will have good performance in presence of uncertainty, because we use the advantages of the SMC and MPC simultaneously.

The reference value of q-axis current based on speed error is shown in Eq. (9). The proof of stability is also presented in Appendix A.

$$\begin{aligned} i_q^* &= \tfrac{1}{a}\left(\omega_e^* + c\omega_e + b\hat{T}_L + k_{swc}\mathrm{sgn}(\omega_e^* - \omega_e)\right) \\ a &= \tfrac{3}{2J_m} Z_p^2 \psi_{mg}\ ,\ b = \tfrac{Z_p}{J_m}\ , c = \tfrac{B_V}{J_m} \\ \mathrm{sgn}(e) &= \begin{cases} +1 & e > 0 \\ -1 & e \le 0 \end{cases} \end{aligned} \tag{9}$$

When the speed error is high enough – during the transient mode – the speed term in C_T will be large and the control scheme behave like a traditional PSC. However, when the actual speed ω_e gets close to the reference value ω_e^*, the current term in C_T will be dominant and penalizes switching combinations that generate high frequencies in the phase currents.

As a result, long prediction horizon is not necessary and the method can be implemented even for topologies with higher complexity like three-level NPC with 27 different switching combinations.

The final task in DPSC design is to determine weighting factors in the cost functions. The weighting factor selection is still an open challenge. However, there are already some proposals in the literature [32]. A simple yet powerful method is the normalization. At this method, first step is to normalize

the errors with different units. After that their values will be determined by heuristic optimization methods or trial and error, by checking the performance of the controller under different situations. At last, the cost function for the proposed PSC to find optimal switching combination is as below:

$$g = C_Z + C_T + C_R \tag{10}$$

4. LOAD TORQUE OBSERVER

Eliminating the sensors used to measure the variables of PMSM increases its reliability and applicability and leads to schemes with more compact constructions and lower costs [33]. Based on Eq. (5) and Eq. (9), the load torque value, T_L, has direct influence on the controller performance. Therefore, a conventional sliding mode observer (SMO) is adopted to accurately and quickly estimate T_L, assuming that the speed sensor is available.

$$\begin{aligned} \dot{\omega}_e &= \frac{Z_p}{J_m}\left(T_e - T_L - \frac{B_v}{Z_p}\omega_e\right) \\ \dot{\hat{\omega}}_e &= \frac{Z_p}{J_m}\left(T_e - \hat{T}_L - \frac{B_v}{Z_p}\hat{\omega}_e\right) \\ e &= \omega_e - \hat{\omega}_e \end{aligned} \tag{11}$$

If we choose $\hat{T}_L$ as Eq. (12), the observer will be stable and reaching speed can be manipulated using k and k_{sw}, the proof is presented in Appendix A;

$$\hat{T}_L = \frac{B_V}{Z_p}e - k_{swo}sgn\,(e) - k_o\,e \tag{12}$$

5. SIMULATION RESULTS

In order to demonstrate the performance of the proposed method, in this section, the proposed method is compared with two other methods reported in [25], as an ordinary direct speed control with one step horizon for two-level back-to-back converter, and [27] that tries to reduce the speed and toque fluctuations by incorporating a current parameter to the objective function. Although there are many works on DPSC strategy for PMSM, they can generally be categorized into two main groups. First one is based on only the speed of PMSM, where [25] is a prestigious work for these methods and second group is based on speed and current (or torque) control, where [27] is one of the best representative for this type of DPSC. The results of some other methods like FOC [3] have been reported in these references and we do not show them here. For summarization, we have compared our results with [25, 27] as the representatives of these two groups, and for comparing to more studies, we refer the reader to the comparisons inside [25, 27]. The following equation shows the tracking terms of [25, 27] where the first term is for [25] and the latter is for [27]. It is worth mentioning that in [27], the current reference value is based on PI controller.

$$\begin{aligned} C_T &= \lambda_\omega * (\omega_e^* - \omega)^2 \quad [25] \\ C_T &= \lambda_\omega * (\omega_e^* - \omega)^2 + \lambda_{iq}\left(i_q^* - i_q\right)^2 \\ i_q^*[k] &= i_q^*[k-1] + k_1\left(\omega_e^*[k] - \omega[k]\right) \\ &\quad + k_2\left(\omega_e^*[k-1] - \omega[k-1]\right) \end{aligned} \Bigg\} \; [27] \tag{13}$$

Table 2 shows all the parameters of the system. The simulations are carried out using MATLAB/Simulink. All simulations are performed using the same parameters, sampling rate and

Table 2. The parameters of the system, controller and observer

System parameters/Symbol		Controller and Observer parameters/Symbol	
R_S	1.3 Ω	λ_{iq}, λ_m	40
L_d, L_q	8 mH	λ_ω	40
ψ_{mg}	0.41 Wb	λ_{Im}	1e6
Z_P	3	λ_{np}	0.5
J_m	0.0212 kg/m^2	k_{swc}	20*b
B_v	3.1e-4 N.ms	k_{swo}	20
C	3 mF	k_o	10
V_{DC}	120	T_m	12 Nm
I_m	2.7	ω_m	400 RPM

observer characteristic. Fig.3 shows the variation of load torque reference and the observer output for actual and estimated value. We have also assumed that there exist inaccuracies about 33% of nominal values of some mechanical system parameters, i.e., J_m and B_v. It can be seen that the observer can estimate the load torque quickly and accurately using the parameters in Table 2.

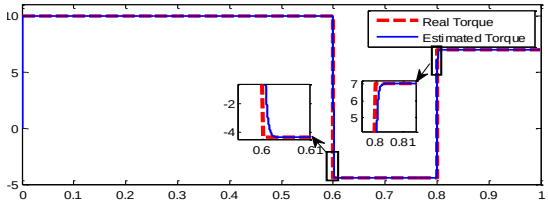

Fig. 3. The load torque real value and observed value.

Fig.4 demonstrates the speed reference, load torque variation and motor speed during the simulation. The reference speed starts from 20 rad/s , at t=1s drops to -20 rad/s and finally at t = 1.405s changes to 10 rad/s. Fig.5 shows some zooms with more details in the results of Fig.4 in different ranges.

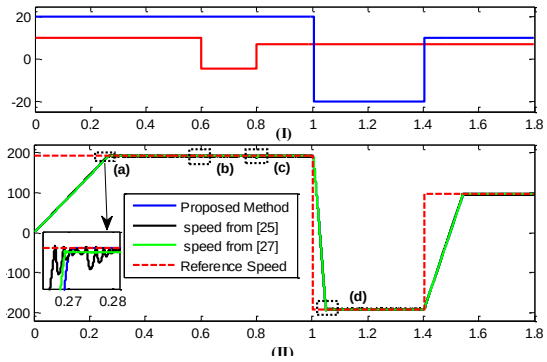

Fig. 4. (I) The reference speed and torque variation during simulation, (II) the reference speed with the system speed responses for different methods.

From Fig.5, it is obvious that PSC of [25] with one step prediction horizon does not show good performance and there is a fluctuation because of the difference between the mechanical and electrical time constant. Unlike [25], the PSC of [27] have almost eliminated fluctuation.

However, its response includes a steady state error. This steady state error is due to the large proportional gain in con-

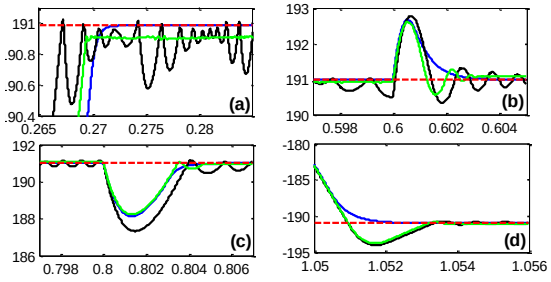

Fig. 5. Zoom in results of Fig.4, the PSC of [25], (solid, black), the PSC of [27] (solid, green) and the proposed method (solid, blue).

trast to the integral gain. Choosing smaller gains may cause the system dynamic to show very slower behavior. Unlike to [25, 27], the proposed method performs a fast and accurate response without oscillations while it uses only one step prediction horizon in its calculation. Utilizing SMO with high stability and robustness properties as well as its quick response due to low computation burden make the proposed method as a strong strategy among the existing works as shown in Figs. 4 and 5.

Fig.6 shows the d-q frame current for aforementioned methods. As it mentioned before and can be seen in this results, in conventional DPSC, q-axis current includes high-frequency components because of considerably large time constant difference between the mechanical and electrical part. The PSC proposed in [27] has a better performance and moderated ripples. However, it fails to eliminate them as much as possible, while the proposed method has very low current distortion compared with the other methods.

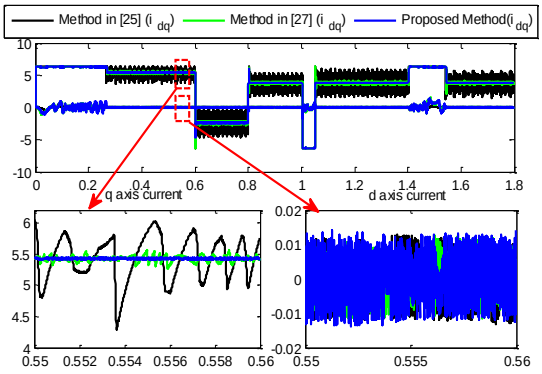

Fig. 6. The d- and q-axis current of the proposed method (blue), the method of [25] (Black) and the method of [27] (green).

To have a quantitative criterion for the current distortion, using Eq. (14), the results are given in Table 3. It can be observed that for i_q, the difference between MSEs are noticeable, but for i_d, they are almost equal. This is due to the fact that in this type of PMSM ($L_d = L_q$), i_d does not have any participation in the speed control and thus controlling i_d is identical for all the mentioned methods.

Table 3. Mean square error of the d- and q- axis currents for t=0.55s to t=0.56s

	PSC from [25]	PSC from [27]	Proposed method
MSE(i_q)	250	4.46	0.08
MSE(i_d)	0.0746	0.0616	0.0859

$$MSE = \sum_{j=1}^{N} \left(i_x(j) - M(i_x) \right)^2$$
$$x = d, q \;\&\; M(i_x) = \frac{\sum_{j=1}^{N} i_x(j)}{N} \quad (14)$$

The electromagnetic torque performance in steady state and transient mode is a very important issue in the motor control, because high ripples in T_e will have unsatisfactory effects on the motor shaft. Fig.7 shows T_e variation over the simulation time. It can be observed that during the transient time, the proposed method have a fast non-oscillatory response. Moreover, it is clear that because of the relation between T_e and i_q, they have the same behavior and all arguments about i_q is also true for T_e in steady state.

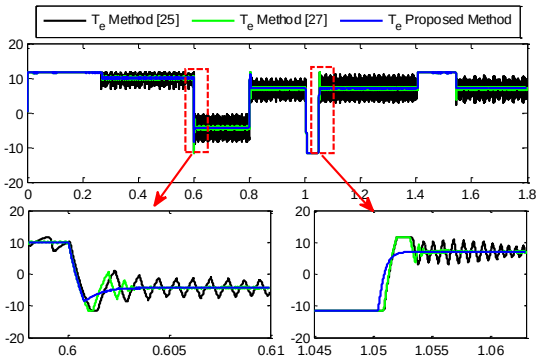

Fig. 7. The torque variation during simulation.

Finally, in Fig.8, d- and q-axis currents, their reference and limitation are illustrated to show that FCS-MPC can successfully manage the current limitation.

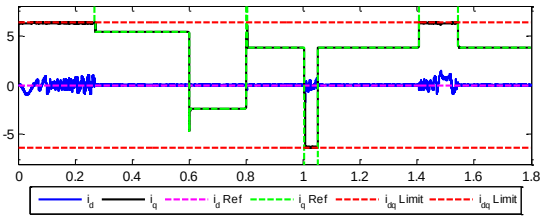

Fig. 8. The d- and q-axis currents with their reference values and limitations.

6. CONCLUSION

In this paper, a DPSC method with one step prediction horizon has been proposed for controlling the speed of PMSM. Since knowing the load torque value has great impact on the controller performance, a simple sliding mode observer is designed to estimate the load torque quickly and accurately.

By considering new reference value of the current into cost function, not only the stability issue is addressed, but also necessity to multiple horizon in PSC is obviated. Furthermore, the effects of the current dynamic on the transient conditions is considered and the controller acts as fast as an original direct speed control without the cascade structure.

The simulation results compared with the existing methods, have shown that the proposed method causes very lower ripple in the current and electromagnetic torque, as an example, for q-axis current it can be seen that the proposed method MSE is about 1.79 percent of PSC from [27] and less than 0.04 percent of the PSC from [25]. Moreover, when the step changes of the speed and load torque applied to system, the proposed controller has fast response with lower overshoot.

In summary, the main advantages of the proposed method compared with the existing methods are as follows. The proposed method uses a direct method with just one step prediction horizon and we need to check less voltage vectors. Therefore, it will consume much less calculation time and lower computation burden compared with other methods and thereby it has shown satisfactory results as shown in the simulation section. Moreover, the proposed method uses sliding mode observer and SMC concepts to generate a reference signal for predictive part. Utilizing a new way for current reference formation like SMC strategy helps us to enhances the stability due to the elimination of outer control loop (as shown in Appendix A). Moreover, SMO increases the robustness of the system against uncertainties and there is no need to use the load torque sensor.

REFERENCES

1. R. Vijayapriya, P. Raja, and M.P. Selvan, “Enhanced method of rotor speed and position estimation of permanent magnet synchronous Machine based on stator SRF-PLL” Engineering Science and Technology, an International Journal, vol 20, no 5, pp 1450-1459, 2017.
2. J.F. Yang and Y.W. Hu, “Optimal direct torque control of permanent magnet synchronous motor”. Proceedings of Chinese Society of Electrical Engineering, vol. 31, pp. 109–115, 2011.
3. J. Holtz, “Advanced PWM and predictive control—An overview,” IEEE Transactions on Industrial Electronics, vol. 63, no. 6, pp. 3837–3844, Jun. 2016.
4. H. Abu-Rub, A. Iqbal, and J. Guzinski, High performance control of ac drives with matlab/simulink models. Chichester, U.K.: Wiley, 2012.
5. A. Linder, R. Kanchan, P. Stolze, and R. Kennel, Model-based predictive control of electric drives. Göttingen, Germany: Cuvillier Verlag, 2012.
6. D. Casdaei, F. Profumo, and G. Serra, “FOC and DTC: two variable schemes for induction motors torque control,” IEEE Transactions on Power Electronics, vol. 17, no. 5, pp. 779-788, 2002.
7. M. F. Rahman, M. E. Haque, and L. X. Tang, “Problems associated with the direct torque control of an interior permanent-magnet synchronous motor drive and their remedies,” IEEE Transactions on Power Electronics, vol. 51, no. 4, pp. 799-809, 2004.
8. M. Sarailoo, B. Rezaie and Z. Rahmani, “Fuzzy predictive control of three-tank system based on a novel modeling framework of hybrid systems”, Proceedings of the Institution of Mechanical Engineering, Part I: Journal of System and Control Engineering, vol. 228, no. 6, pp. 369-384, 2014.
9. F. Rajabi, B. Rezaie and Z. Rahmani, “Designing NMPC controller using hybrid PSO-SQP algorithm: Application to an evaporator system”, Transactions of the Institute of Measurement and Control, vol. 38, no. 1, pp. 23-32, 2016.
10. S. Jalili, B. Rezaie and Z. Rahmani, “A novel hybrid model predictive control design with application to a quadrotor helicopter”, Optimal Control Applications and Methods, vol. 39, no. 4, pp. 1301-1322, 2018.
11. M.R. Zamani, Z. Rahmani and B. Rezaie, “A novel model predictive control for a piecewise affine class of hybrid system with repetitive disturbance,” ISA Transactions, 2020. DOI: https://doi.org/10.1016/j.isatra.2020.08.023
12. J. Bocker, B. Freudenberg, A. The, and S. Dieckerhoff, “Experimental comparison of model predictive control and cascaded control of the modular multilevel converter,” IEEE Transactions on Power Electronics, vol. 30, no. 1, pp. 422–430, Jan. 2015.
13. H. Abu-Rub, J. Guzinski, Z. Krzeminski, and H. A. Toliyat, “Predictive current control of voltage-source inverters,” IEEE Transactions on Industrial Electronics, vol. 51, no. 3, pp. 585–593, Jun. 2004.
14. F. Wang, X. Mei, J. Rodriguez and R. Kennel, “Model predictive control for electrical drive systems-an overview,” CES Transactions on Electrical Machines and Systems, vol. 1, no. 3, pp. 219-230, Sept. 2017.
15. Liuping Wang, Lu Gan, “Integral FCS Predictive Current Control of Induction Motor Drive,” IFAC Proceedings Volumes, vol. 47, no. 3, pp. 11956-11961, 2014.
16. T. Dragičević, “Dynamic stabilization of DC microgrids with predictive control of point-of-load converters,” IEEE Transactions on Power Electronics, vol. 33, no. 12, pp. 10872-10884, Dec. 2018.
17. O. Sandre-Hernandez, J. Rangel-Magdaleno and R. Morales-Caporal, "A comparison on finite-set model predictive torque control schemes for PMSMs," in IEEE Transactions on Power Electronics, vol. 33, no. 10, pp. 8838-8847, Oct. 2018.
18. R. Vargas, J. Rodriguez, U. Ammann, and P. Wheeler, “Predictive current control of an induction machine fed by a matrix converter with reactive power control,” IEEE Transactions on Industrial Electronics, vol. 55, no. 12, pp. 4362– 4371, Dec. 2008.
19. F. Ban, G. Lian, J. Zhang, B. Chen and G. Gu, “Study on a novel predictive torque control strategy based on the finite control set for PMSM,” IEEE Transactions on Applied Superconductivity, vol. 29, no. 2, pp. 1-6, Mar. 2019.
20. J. Rodriguez, R. Kennel, J. Espinoza, M. Trincado, C. Silva, and C. Rojas, “High-performance control strategies for electrical drives: An experimental assessment,” IEEE Transactions on Industrial Electronocs, vol. 59, no. 2, pp. 812–820, Feb. 2012.
21. S. Chai, L. Wang, and E. Rogers, “A cascade MPC control structure for a PMSM with speed ripple minimization,” IEEE Trans. Industrial Electronics, vol. 60, no. 8, pp. 2978–2987, Aug. 2013
22. E. Fuentes, C. Silva, D. Quevedo, and E. Silva, “Predictive speed control of a synchronous permanent magnet motor,” in Proceedings of IEEE ICIT, Feb. 2009.
23. E. J. Fuentes, C. A. Silva and J. I. Yuz, “Predictive speed control of a two-mass system driven by a permanent magnet synchronous motor”, IEEE Transactions on Industrial Electronics, vol. 59, no. 7, pp. 2840-2848, Jul. 2012.
24. E. Fuentes, D. Kalise, J. Rodríguez and R. M. Kennel, “Cascade-free predictive speed control for electrical drives,” IEEE Transactions on Industrial Electronics, vol. 61, no. 5, pp. 2176-2184, May 2014.
25. M. Preindl and S. Bolognani, “Model predictive direct speed control with finite control set of PMSM drive systems,” IEEE Transactions on Power Electronics, vol. 28, no. 2, pp. 1007–1015, Feb. 2013.
26. L. Wang, S. Chai, D. Yoo, L. Gan, and K. Ng, PID and predictive control of electrical drives and power converters using matlab/simulink. Hoboken, NJ, USA: Wiley, 2015.
27. P. Kakosimos and H. Abu-Rub, “Predictive Speed Control With Short Prediction Horizon for Permanent Magnet Synchronous Motor Drives,” IEEE Transactions on Power Electronics, vol. 33, no. 3, pp. 2740-2750, March 2018.
28. N. Kazantzis and C. Kravaris, “Time-discretization of nonlinear control systems via Taylor methods,” Computers & Chemical Engineering, vol. 23, no. 6, pp. 763-784, Jan. 1999
29. Z. Zhang, F. Wang, J. Wang, J. Rodríguez and R. Kennel, “Nonlinear direct control for three-level NPC back-to-back converter PMSG wind turbine systems: experimental assessment with FPGA,” in IEEE Transactions on Industrial Informatics, vol. 13, no. 3, pp. 1172-1183, June 2017.
30. S. Bolognani, R. Petrella, A. Prearo, and L. Sgarbossa, “Automatic tracking of MTPA trajectory in ipm motor drives based on ac current

injection," in Proceedings of IEEE Energy Conversion. Congr. Expo., 2009, pp. 2340–2346.
31. K. Li and Y. Wang, "Maximum torque per ampere (MTPA) control for IPMSM drives based on a variable-equivalent-parameter MTPA control law," IEEE Transactions on Power Electronics, vol. 34, no. 7, pp. 7092-7102, July 2019.
32. P. Cortes, S. Kouro, B. La Rocca, R. Vargas, J. Rodriguez, J. I. Leon, S. Vazquez, and L.G. Franquello, "Guidelines for weighting factors design in model predictive control of power converters and drives," in Proceedings of IEEE International Conference on Industrial Technology, 2009.
33. S. Saberi and B. Rezaie, "A full range permanent magnet synchronous motor position and speed estimation using adaptive non-singular fast terminal sliding mode observer," Majlesi Journal of Energy Management, vol. 8, no. 4, pp. 17-25, 2019.

APPENDIX A

The load torque observer stability proof:

Consider the speed dynamic estimation as Eq. (15):

$$\dot{\hat{\omega}}_e = \frac{Z_p}{J_m}\left(T_e - \hat{T}_L - \frac{B_v}{Z_p}\hat{\omega}_e\right) \tag{15}$$

$\hat{T}_L$ is the estimation of the load torque or the lumped sum disturbance. Consider the error of speed estimation as:

$$e_1 = \omega_e - \hat{\omega}_e \tag{16}$$

By selecting a simple quadratic Lyapunov function and derivating it, we have:

$$\begin{aligned} &V = \tfrac{1}{2}e_1^2 \Rightarrow \dot{V} = e_1\dot{e}_1 = e_1\tfrac{Z_p}{J_m}\left(-\tfrac{B_v}{Z_p}\left(\omega_e - \hat{\omega}_e\right) - T_L + \hat{T}_L\right) \\ &\dot{V} = e_1\tfrac{Z_p}{J_m}\left(-\tfrac{B_v}{Z_p}e_1 - T_L + \hat{T}_L\right) \end{aligned} \tag{17}$$

If we choose $\hat{T}_L$ as Eq. (18):

$$\hat{T}_L = \frac{B_v}{Z_p}e_1 - k_{swo}\mathrm{sgn}\left(e_1\right) - k_o e_1 \tag{18}$$

By substituting Eq. (18) into Eq. (17), the derivative of Lyapunov function is:

$$\begin{aligned} \dot{V} &= e_1\tfrac{Z_p}{J_m}\left(-k_{swo}\mathrm{sgn}\left(e_1\right) - k_o e_1 - T_L\right) \\ &= \tfrac{Z_p}{J_m}\left(-k_o e_1^2 - k_{swo}\left|e_1\right| - T_L e_1\right) \\ &\Rightarrow \dot{V} \le \tfrac{Z_p}{J_m}\left(-k_o e_1^2 - k_{swo}\left|e_1\right| + \left|T_L\right|\left|e_1\right|\right) \end{aligned} \tag{19}$$

By considering that T_L is bounded, i.e., $T_L \le D_1$, then:

$$\begin{aligned} \dot{V} &\le \tfrac{Z_p}{J_m}\left(-k_o e_1^2 - k_{swo}\left|e_1\right| + D_1\left|e_2\right|\right) \\ &= \tfrac{Z_p}{J_m}\left(-k_o e_1^2 - \left(k_{swo} - D_1\right)\left|e_1\right|\right) \\ &if\ k_{swo} > D_1 > 0\ \&\ k_o > 0 \Rightarrow \dot{V} < 0 \end{aligned} \tag{20}$$

The current reference value evaluation and stability proof:

For the electrical speed dynamic, we rewrite Eq. (1) as:

$$\dot{\omega}_e = ai_q - bT_L - c\omega_e \tag{21}$$

where a, b and c are introduced in Eq. (9). By considering the error as $e_2 = \omega_e^* - \omega_e$ and Lyapunov function as $V = 1/2\left(e_2^2\right)$, while assuming that T_L is observed using observer, we should design i_q that way $\dot{V} \le 0$ and $\dot{V}\left(0\right) = 0$.

$$\dot{V} = e_2\dot{e}_2 = e_2\left(\dot{\omega}_e^* - \dot{\omega}_e\right) = e_2\left(\dot{\omega}_e^* - ai_q + bT_L + c\omega_e\right) \tag{22}$$

If we choose i_q as Eq. (9), then $\dot{V}$ becomes:

$$\dot{V} = e_2\left(-k_{swc}\mathrm{sgn}(e_2)\right) = -k_{swc}\left|e_2\right| - k_{swc}be_2\underbrace{\left(\hat{T}_L - T_L\right)}_{\tilde{T}_L} \tag{23}$$

where $\tilde{T}_L$ is the observer error. From Eq. (20), we know that this variable is bounded, i.e., $\tilde{T}_L \le D_2$ Thus, we can write:

$$\begin{aligned} \dot{V} &\le -k_{swc}\left|e_2\right| + bk_{swc}\left|e_2\right|\left|\tilde{T}_L\right| \\ &\le -k_{swc}\left|e_2\right| + bk_{swc}\left|e_2\right|D_2 \\ &= -\left(k_{swc} - bD_2\right)\left|e_2\right| \end{aligned} \tag{24}$$

If $k_{swc} > bD_2$, then $\dot{V} \le 0$. It should be noted that if $e_2 = 0$, then $\dot{V} = 0$.